Inverse Scattering of Inhomogeneous Biaxial Materials Coated on a Conductor

Chien-Ching Chiu

***Abstract*— The inverse scattering of inhomogeneous biaxial materials coated on a perfectly conducting cylinder with known cross section is investigated. A group of unrelated incident waves is used to illuminate the cylinder. By properly arranging the direction and polarization of various unrelated incident waves, the difficulties of ill-posedness and nonlinearity were circumvented and the permittivity tensor distribution can be reconstructed through simple matrix operations. For theoretical formulation based on the boundary condition, a set of integral equations is derived and solved by the moment method as well as the unrelated illumination method. Numerical results show that the permittivity tensor distribution of the materials can be successfully reconstructed even when the permittivity is fairly large. Good reconstruction has been obtained both with and without Gaussian noise in measured data. In addition, the effect of noise contamination on imaging is also examined.**

***Index Terms*—Electromagnetic scattering, inverse problems.**

I. Introduction

ADVANCED composite materials are increasingly popular in industrial and military application due to their superior properties in strength, stiffness, fatigue resistance, and low thermal expansion. Laminated composite materials are widely used to coat on the metal and the aircraft. The electromagnetic inverse scattering of advanced composite materials coated on conductors has been a subject of considerable importance in various area of technology. However, the solution of this problem is very complicated and difficult due to the following reasons.

1) The inverse scattering problem is nonlinear in nature because it involves the product of two unknowns, the electrical property of the object, and the electric field within the object. This problem is also ill-posed due to the fact that the kernel of the integral is a smoothing function.
2) Advanced composite materials are electrically anisotropic. The permittivity of this materials depends on the chosen coordinates. Thus, this problem is more difficult and complex than that of isotropic materials.
3) This problem involves both conductor and biaxial dielectric materials at the same time. To our knowledge, there is still no rigorous algorithm for such cases.

Rigorous algorithms, which solved the exact integral equation by numerical method, have been developed during the last two decades. Ney *et al.* [1] and Caorsi *et al.* [2] use the inverse source method and the pseudo-inverse transformation technique to solve the inverse problem. Some modification of inverse source method with basis functions expansion for nonradiating current was proposed by Habashy and Oristaglio [3]. Note that the major difficulty of the inverse source method is the ill-posedness in inverting the matrix corresponding the integral of the Green function. Based on the idea that sufficient information may be obtained by arranging various unrelated incident waves. An "unrelated illumination method" [4], [5] was proposed by Wang and Zhang [4] on the inverse scattering problem. In their method, the only matrix being inverted is the one corresponding to the incident waves. Thus, the difficulties of the ill-posedness and nonlinearity are circumvented. Good reconstruction was obtained through simple matrix operations. An iterative algorithm based on the Newton–Kantorovitch method with Tikhonov regularization was proposed by Joachimowicz *et al.* [6]. The simulated results show that ill-posedness can be reduced by enforcing the convergence with *a priori* information. Some algorithms based on the optimization procedure that avoid the necessity of solving a direct problem at each step of iteration have also been proposed [7]–[9].

In this paper, the inverse scattering of advanced composite biaxial materials coated on a conductor is investigated. An

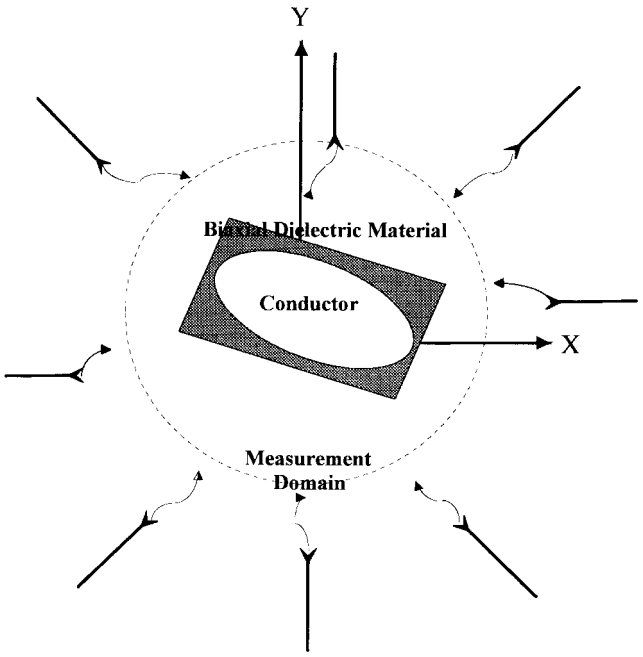

Fig. 1. Geometry of the problem in the (x, y) plane.

Manuscript received July 30, 1996; revised July 28, 1997. This work was supported by the National Science Council, ROC under Grant NSC 85-2213-E032-001.

The author is with the Department of Electrical Engineering, Tamkang University, Tamsui, Taiwan, ROC.

Publisher Item Identifier S 0018-926X(98)01490-2.

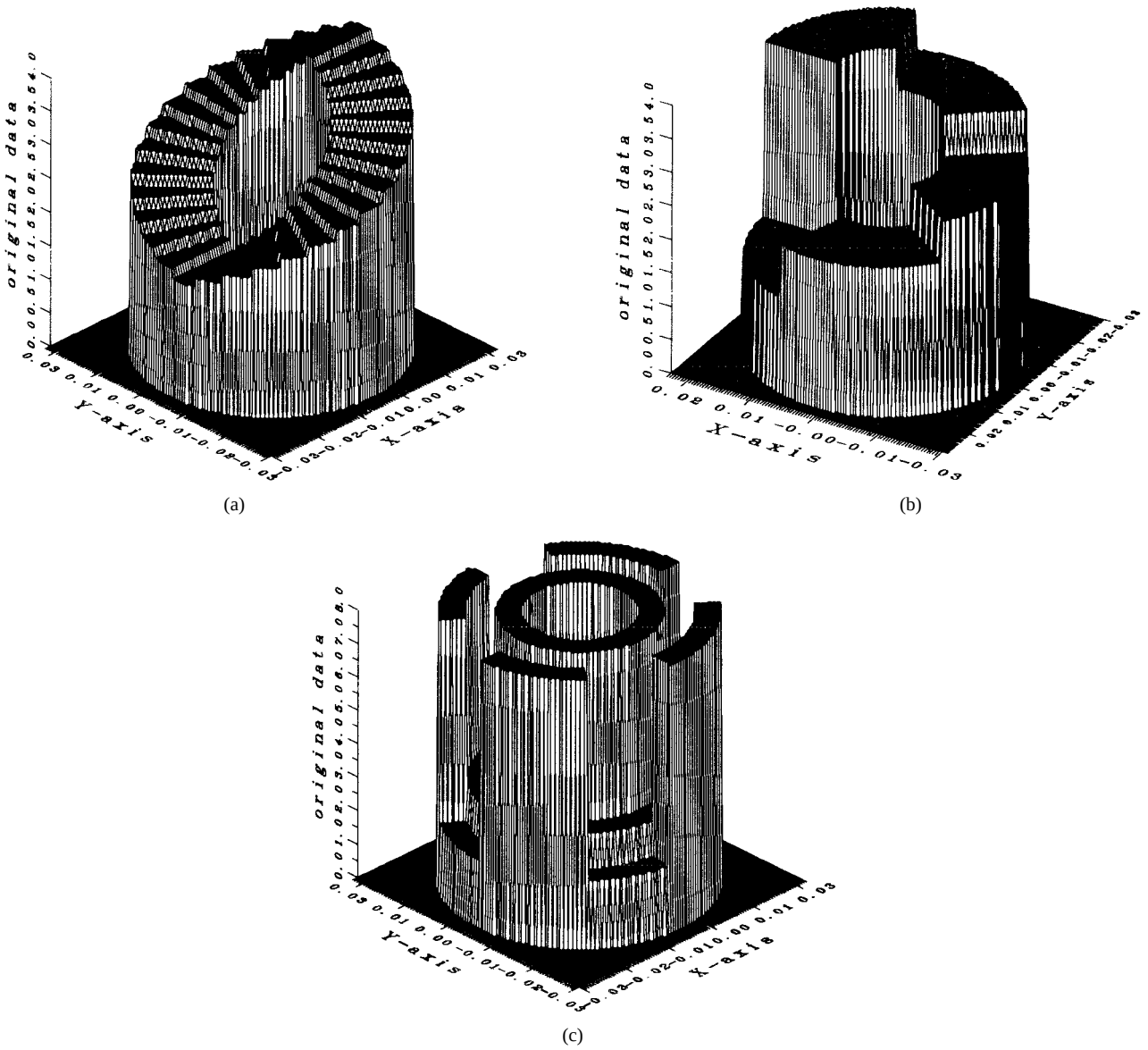

Fig. 2. Original relative permittivity tensor distribution for example 1. (a) $\varepsilon_1(x, y)$. (b) $\varepsilon_2(x, y)$. (c) $\varepsilon_3(x, y)$.

efficient algorithm is proposed to recover the permittivity distribution of the materials by using the knowledge of the shape of the conductor and the scattered field measured outside. This algorithm is based on the unrelated illumination method [4] and the moment method [10]. In Section II, the theoretical formulation for electromagnetic scattering is presented. We introduce some techniques to overcome ill-posedness. Numerical results for biaxial cylinders of different permittivities and different cross sections are given in Section III. Finally, some conclusions are drawn in Section IV.

II. Theoretical Formulation

A. Direct Problem

Let us consider a cylindrical complex object which consists of inhomogeneous biaxial dielectric materials and the perfect conductor in free-space, as shown in Fig. 1. Assume that the complex object is infinitely extended in the z direction and the biaxial materials are inhomogeneous in x–y plane, i.e., only two-dimensional (2-D) case is considered. The permeability of the materials are μ_0 and the relative permittivity tensors $\overline{\overline{\varepsilon}}_r$ of the materials are represented by diagonal matrix in the Cartesian coordinate system

$$\overline{\overline{\varepsilon}}_r(x, y) = \begin{bmatrix} \varepsilon_1(x, y) & 0 & 0 \\ 0 & \varepsilon_2(x, y) & 0 \\ 0 & 0 & \varepsilon_3(x, y) \end{bmatrix}_{xyz}.$$

The elements in $\overline{\overline{\varepsilon}}_r$ are dimensionless and are complex in the general case. Here, the permittivity tensors $\overline{\overline{\varepsilon}}_r(r)$ are to be constructed in our inverse scattering problem with *a priori* knowledge of the conductor's shape. The object is illuminated by the following two different polarized incident waves.

1) TM Waves: Let $\overline{E}^i = E_z^i \hat{z}$ denote the incident wave. Then the integral equation for the internal total field inside the

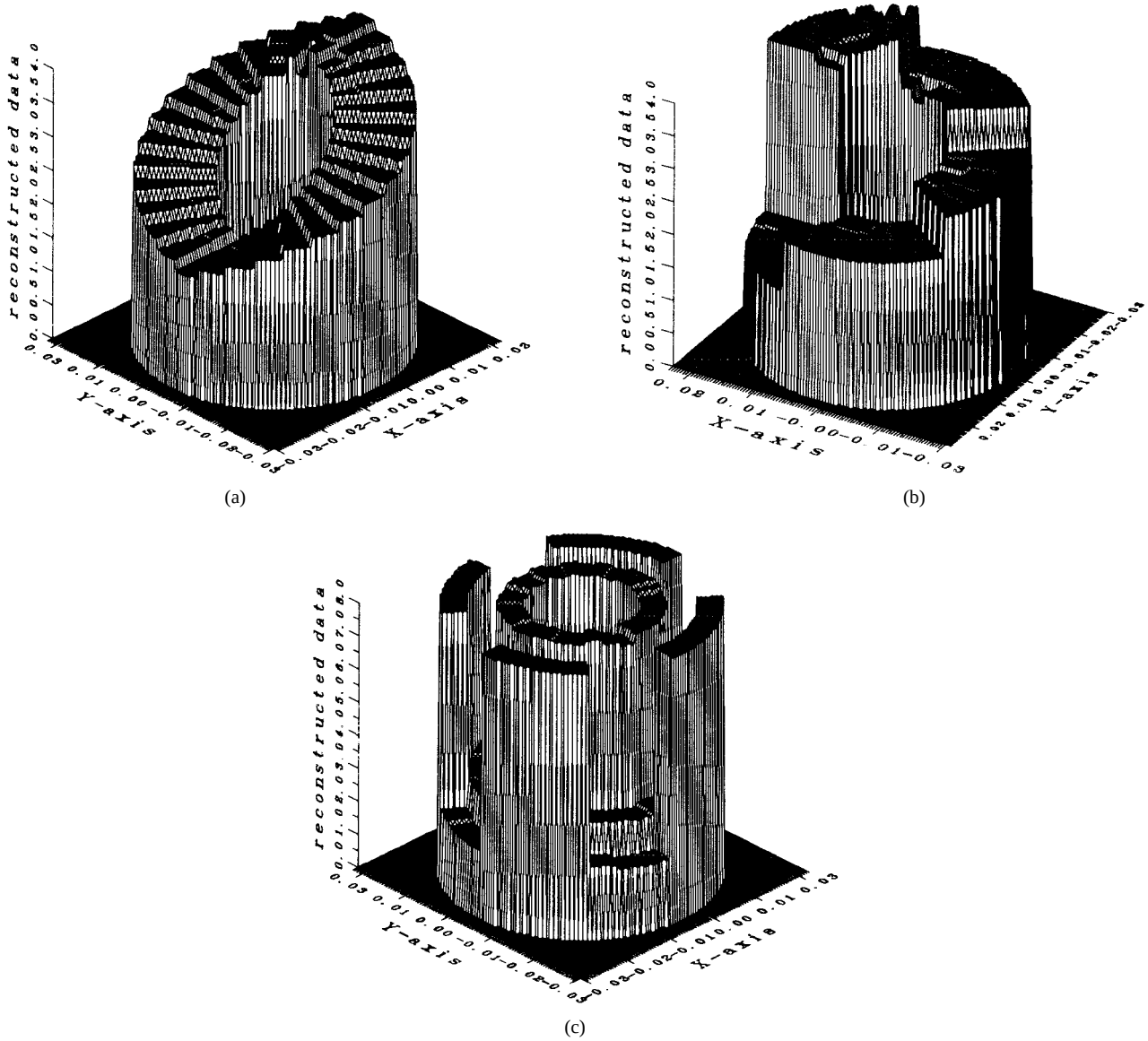

Fig. 3. Reconstructed relative permittivity tensor distribution for example 1. (a) $\varepsilon_1(x, y)$. (b) $\varepsilon_2(x, y)$. (c) $\varepsilon_3(x, y)$.

biaxial materials can be expressed by [11]

$$-E_z^i(\overline{r}) = \int_s G(\overline{r}, \overline{r}')k_0^2[\varepsilon_3(\overline{r}') - 1]E_z(\overline{r}')\, ds' - j\omega\mu_0 \int_c G(\overline{r}, \overline{r}')J_s(\overline{r}')\, dl' - E_z(\overline{r}) \quad (1)$$

where k_0 denotes the free-space wavenumber. J_s is the induced electric surface current density which is proportional to the normal derivative of the electric field on the conductor surface. S represents the area of the dielectric materials and C is the contour of the conductor. $G(\overline{r}, \overline{r}')$ is 2-D Green function for free-space and can be expressed as

$$G(\overline{r}, \overline{r}') = -\frac{j}{4} H_0^{(2)}(k_0|\overline{r} - \overline{r}'|)$$

where $H_0^{(2)}$ is the Hankel function of the second kind of order zero.

The boundary condition states that the total tangential electric field must be zero on the surface of the perfectly conducting cylinder and this yields the following equation:

$$-E_z^i(\overline{r}) = \int_s G(\overline{r}, \overline{r}')k_0^2[\varepsilon_3(\overline{r}') - 1]E_z(\overline{r}')\, ds' - j\omega\mu_0 \int_c G(\overline{r}, \overline{r}')J_s(\overline{r}')\, dl'. \quad (2)$$

The external scattered field is given by

$$E_z^s(\overline{r}) = \int_s G(\overline{r}, \overline{r}')k_0^2[\varepsilon_3(\overline{r}') - 1]E_z(\overline{r}')\, ds' - j\omega\mu_0 \int_c G(\overline{r}, \overline{r}')J_s(\overline{r}')\, dl'. \quad (3)$$

2) TE Waves:

Incident waves $\overline{E}^i = E_x^i\hat{x} + E_y^i\hat{y}$ are incident upon the object. Owing to the coupling between E_x and E_y, the equations governing the result total field in the TE case are more complicated than those in the TM case. By equivalent induced

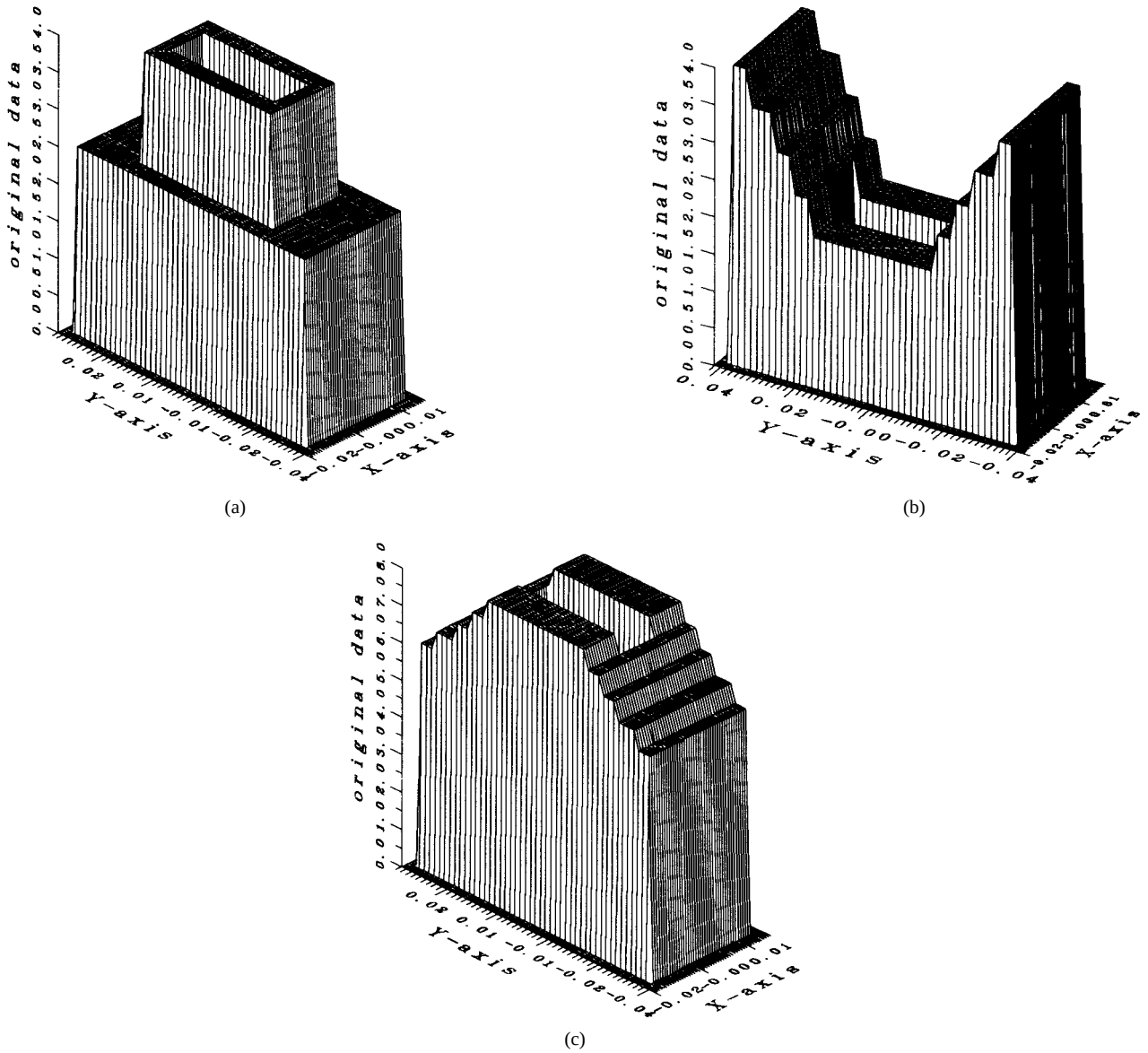

Fig. 4. Original relative permittivity tensor distribution for example 2. (a) $\varepsilon_1(x, y)$. (b) $\varepsilon_2(x, y)$. (c) $\varepsilon_3(x, y)$.

current concept and Hertz vectorial potential techniques [11], the integral equation for the internal total field $\overline{E} = E_x\hat{x} + E_y\hat{y}$ inside the biaxial materials can be express as follows:

$$-E_x^i(\overline{r}) = \left(\frac{\partial^2}{\partial x^2} + k_0^2\right)\left\{\int_s G(\overline{r}, \overline{r}')[\varepsilon_1(\overline{r}') - 1]E_x(\overline{r}')\,ds'\right\} + \frac{\partial^2}{\partial x\,\partial y}\left\{\int_s G(\overline{r}, \overline{r}')[\varepsilon_2(\overline{r}') - 1]E_y(\overline{r}')\,ds'\right\} + \frac{\partial}{\partial y}\left[\int_c G(\overline{r}, \overline{r}')J_{sm}(\overline{r}')\,dl'\right] - E_x(\overline{r}) \tag{4}$$

$$-E_y^i(\overline{r}) = \frac{\partial^2}{\partial x\,\partial y}\left\{\int_s G(\overline{r}, \overline{r}')[\varepsilon_1(\overline{r}') - 1]E_x(\overline{r}')\,ds'\right\} + \left(\frac{\partial^2}{\partial y^2} + k_0^2\right)\left\{\int_s G(\overline{r}, \overline{r}')[\varepsilon_2(\overline{r}') - 1]E_y(\overline{r}')\,ds'\right\} - \frac{\partial}{\partial x}\left[\int_c G(\overline{r}, \overline{r}')J_{sm}(\overline{r}')\,dl'\right] - E_y(\overline{r}) \tag{5}$$

where J_{sm} is equivalent magnetic surface current density in the z direction. According to the boundary condition on the surface of the conductor, the following integral equation is obtained:

$$\begin{aligned}-\hat{n}\times[E_x^i(\overline{r})\hat{x} + E_y^i(\overline{r})\hat{y}] &= \hat{n}\times\left[\left(\left(\frac{\partial^2}{\partial x^2} + k_0^2\right)\left\{\int_s G(\overline{r}, \overline{r}')[\varepsilon_1(\overline{r}') - 1]E_x(\overline{r}')\,ds'\right\}\right.\right. \\ &\quad + \frac{\partial^2}{\partial x\,\partial y}\left\{\int_s G(\overline{r}, \overline{r}')[\varepsilon_2(\overline{r}') - 1]E_y(\overline{r}')\,ds'\right\} \\ &\quad \left. + \frac{\partial}{\partial y}\int_c G(\overline{r}, \overline{r}')J_{sm}(\overline{r}')\,dl'\right)\hat{x} \\ &\quad + \left(\frac{\partial^2}{\partial x\,\partial y}\left\{\int_s G(\overline{r}, \overline{r}')[\varepsilon_1(\overline{r}') - 1]E_x(\overline{r}')\,ds'\right\}\right. \\ &\quad + \left(\frac{\partial^2}{\partial y^2} + k_0^2\right)\left\{\int_s G(\overline{r}, \overline{r}')[\varepsilon_2(\overline{r}') - 1]E_y(\overline{r}')\,ds'\right\} \\ &\quad \left.\left. - \frac{\partial}{\partial x}\int_c G(\overline{r}, \overline{r}')J_{sm}(\overline{r}')\,dl'\right)\hat{y}\right]\end{aligned} \tag{6}$$

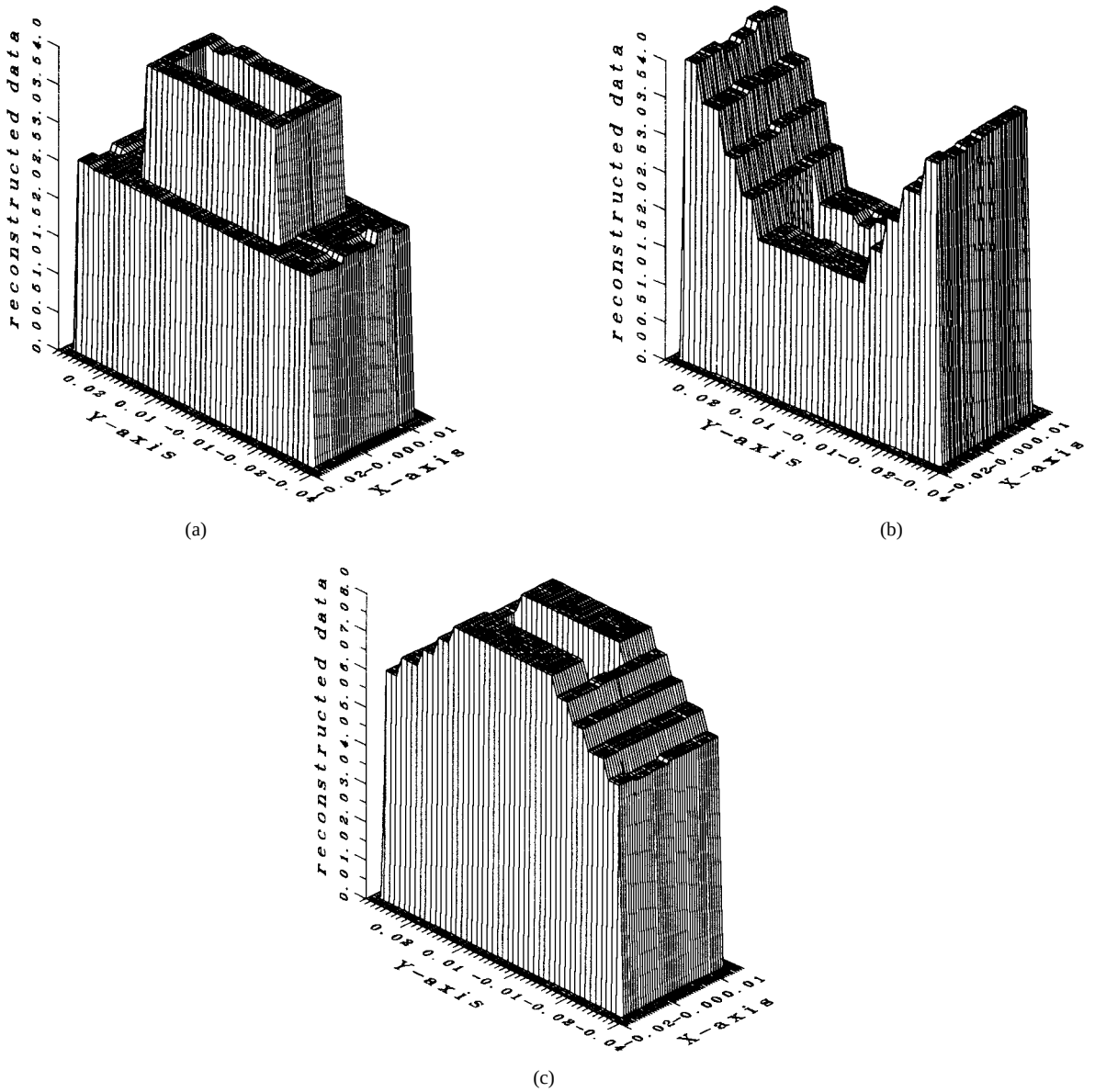

Fig. 5. Reconstructed relative permittivity tensor distribution for example 2. (a) $\varepsilon_1(x, y)$. (b) $\varepsilon_2(x, y)$. (c) $\varepsilon_3(x, y)$.

where $\hat{n}$ is the outward unit vector normal to the surface of the conductor. $\hat{x}$ and $\hat{y}$ are unit vectors aligned along the x and y axes in positive directions. The external scattered field can be expressed by

$$E_x^s(\overline{r}) = \left(\frac{\partial^2}{\partial x^2} + k_0^2\right)\left\{\int_s G(\overline{r}, \overline{r}')[\varepsilon_1(\overline{r}') - 1]E_x(\overline{r}')\, ds'\right\} + \frac{\partial^2}{\partial x\, \partial y}\left\{\int_s G(\overline{r}, \overline{r}')[\varepsilon_2(\overline{r}') - 1]E_y(\overline{r}')\, ds'\right\} + \frac{\partial}{\partial y}\left\{\int_c G(\overline{r}, \overline{r}')J_{sm}(\overline{r}')\, dl'\right\} \quad (7)$$

$$E_y^s(\overline{r}) = \frac{\partial^2}{\partial x\, \partial y}\left\{\int_s G(\overline{r}, \overline{r}')[\varepsilon_1(\overline{r}') - 1]E_x(\overline{r}')\, ds'\right\} + \left(\frac{\partial^2}{\partial y^2} + k_0^2\right)\left\{\int_s G(\overline{r}, \overline{r}')[\varepsilon_2(\overline{r}') - 1]E_y(\overline{r}')\, ds'\right\} - \frac{\partial}{\partial x}\left\{\int_c G(\overline{r}, \overline{r}')J_{sm}(\overline{r}')\, dl'\right\}. \quad (8)$$

For the direct problem, the scattered field is computed by giving the permittivity distribution of the biaxial materials and the shape of the conductor. This can be achieved by using (1), (2), and (4)–(6) to solve the total field inside the materials $\overline{E}$, the induced electric surface current density J_s, and the equivalent magnetic surface density J_{sm} and then calculating $\overline{E}^s$ by (3), (7), and (8). For numerical implementation of the direct problem, the dielectric materials are divided into N_1 sufficient small cells. Thus, the permittivity and the total field within each cell can be taken as constants. Similarly, we divide the contour of the conductor into N_2 sufficient small segments so that the induced electric and equivalent magnetic surface current density can be considered constant over each segment. Let ε_{1n}, ε_{2n}, and ε_{3n} denote the x, y, and z component of the relative permittivity in the nth cell. In application of the moment method, pulse functions for expansion and point matching for testing [10] are used to solve (1)–(8). Thus, the

following matrix equations can be obtained:

$$-(E_z^i) = ([G_1][\tau_3] - [I])(E_z) + [G_2](J_s) \tag{9}$$

$$-(E_v^i) = [G_3][\tau_3](E_z) + [G_4](J_s) \tag{10}$$

$$(E_z^s) = [G_5][\tau_3](E_z) + [G_6](J_s) \tag{11}$$

$$\begin{pmatrix} -E_x^i \\ -E_y^i \end{pmatrix} = \left\{ \begin{bmatrix} [G_7] & [G_8] \\ [G_8] & [G_{10}] \end{bmatrix} \begin{bmatrix} [\tau_1] & 0 \\ 0 & [\tau_2] \end{bmatrix} - \begin{bmatrix} [I] & 0 \\ 0 & [I] \end{bmatrix} \right\} \cdot \begin{pmatrix} E_x \\ E_y \end{pmatrix} + \begin{bmatrix} [G_9] \\ [G_{11}] \end{bmatrix} (J_{sm}) \tag{12}$$

$$-(E_h^i) = [G_{12}][\tau_1] + [G_{13}][\tau_2] + [G_{14}](J_{sm}) \tag{13}$$

$$\begin{pmatrix} E_x^s \\ E_y^s \end{pmatrix} = \begin{bmatrix} [G_{15}] & [G_{16}] \\ [G_{16}] & [G_{18}] \end{bmatrix} \begin{bmatrix} [\tau_1] & 0 \\ 0 & [\tau_2] \end{bmatrix} \begin{pmatrix} E_x \\ E_y \end{pmatrix} + \begin{bmatrix} [G_{17}] \\ [G_{19}] \end{bmatrix} (J_{sm}) \tag{14}$$

where (E_x), (E_y), and (E_z) represent the N_1 element total field column vectors and (E_x^i), (E_y^i), and (E_z^i) are the N_1 element incident field column vectors. (E_v^i) and (E_h^i) are the N_2 element column vectors. (E_x^s), (E_y^s), and (E_z^s) denote the M element scattered field column vectors. Here, M is the number of measurement points. (J_s) and (J_{sm}) are the N_2 element column vectors. The matrices $[G_1]$, $[G_7]$, $[G_8]$, and $[G_{10}]$ are $N_1 \times N_1$ square ones. $[G_2]$, $[G_9]$, and $[G_{11}]$ are $N_1 \times N_2$ matrices. $[G_3]$, $[G_{12}]$, and $[G_{13}]$ are $N_2 \times N_1$ matrices. $[G_4]$ and $[G_{14}]$ are $N_2 \times N_2$ square matrices. $[G_5]$, $[G_{15}]$, $[G_{16}]$, and $[G_{18}]$ are $M \times N_1$ matrices. $[G_6]$, $[G_{17}]$, and $[G_{19}]$ are $M \times N_2$ matrices. The elements in matrices $[G_i]$— $i = 1, 2 \cdots 19$—can be obtained by tedious mathematic manipulation. $[\tau_1]$, $[\tau_2]$, and $[\tau_3]$ are $N_1 \times N_1$ diagonal matrices, their diagonal elements are given as follows:

$$[\tau_i]_{nn} = \varepsilon_{in}(x, y) - 1, \qquad i = 1, 2, 3$$

and $[I]$ is a $N_1 \times N_1$ identity matrix. We can solve the direct problem for the TM case by using (9)–(11). Similarly, the direct problem for the TE case can be solved by using (12)–(14).

2) Inverse Problem: Now, we consider the following inverse problem; given the shape of the conductor and the scattered field measured outside, determine the permittivity distribution of the biaxial materials. Note that the only unknown permittivity in the TM case is $\varepsilon_3(\overline{r})$, and $\varepsilon_1(\overline{r})$ as well as $\varepsilon_2(\overline{r})$ in the TE case.

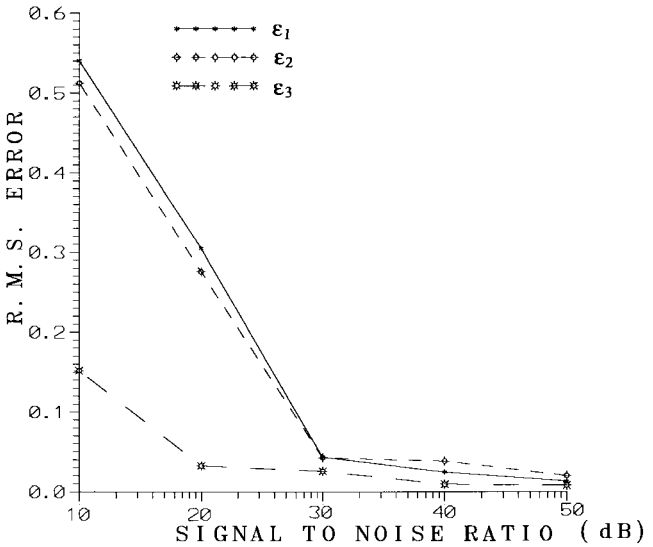

Fig. 6. Reconstructed error as a function of SNR for Example 1.

For solving the inverse problem, we first calculate (J_s) by (10) and (J_{sm}) by (13), and then substitute (J_s) into (9) and (11) as well as (J_{sm}) into (12) and (14). Next, N_1 different incident column vectors for the TM case and $2N_1$ different incident column vectors for the TE case are used to illuminate the object, the following equations can be obtained:

$$-[E_p^i] = ([G_{p1}][\tau_3] - [I])[E_z] \tag{15}$$

$$[E_p^s] = [G_{p2}][\tau_3][E_z] \tag{16}$$

$$-[E_t^i] = ([G_{t1}][\tau_t] - [I_t])[E_t] \tag{17}$$

$$[E_t^s] = [G_{t2}][\tau_t][E_t] \tag{18}$$

where given in the equation at the bottom of the page.

Here, $[E_p^i]$ is a $N_1 \times N_1$ square matrix and $[E_p^s]$ is a $M \times N_1$ matrix. $[E_t^i]$ and $[E_t^s]$ are $2N_1 \times 2N_1$ and $M \times 2N_1$ matrices, respectively. Note that the matrices $[G_4]$ and $[G_{14}]$ are diagonally dominant and always invertible. It is worth mentioning that other than the matrices $[G_{p2}]$ and $[G_{t2}]$, the matrices $[G_{p1}][\tau_3] - [I]$ and $[G_{t1}][\tau_t] - [I_t]$ is always well-posed ones in any case. Therefore, by first solving $[E_z]$ in (15) as well as $[E_t]$ in (17), and substituting into (16) and (18), respectively. Then $[\tau_3]$ and $[\tau_t]$ can be found by solving

$$[E_p^i] = [E_z^i] - [G_2][G_4]^{-1}[E_v^i] \quad [E_p^s] = [E_z^s] + [G_6][G_4]^{-1}[E_v^i]$$

$$[G_{p1}] = [G_1] - [G_2][G_4]^{-1}[G_3] \quad [G_{p2}] = [G_5] - [G_6][G_4]^{-1}[G_3]$$

$$[E_t^i] = \begin{bmatrix} E_x^i - [G_9][G_{14}]^{-1}(E_h^i) \\ E_y^i - [G_{11}][G_{14}]^{-1}(E_h^i) \end{bmatrix} \quad [E_t^s] = \begin{bmatrix} E_x^s + [G_{17}][G_{14}]^{-1}(E_h^i) \\ E_y^s + [G_{19}][G_{14}]^{-1}(E_h^i) \end{bmatrix}$$

$$[G_{t1}] = \begin{bmatrix} [G_7] - [G_9][G_{14}]^{-1}[G_{12}] & [G_8] \\ [G_8] & [G_{10}] - [G_{11}][G_{14}]^{-1}[G_{13}] \end{bmatrix}$$

$$[G_{t2}] = \begin{bmatrix} [G_{15}] - [G_{17}][G_{14}]^{-1}[G_{12}] & [G_{16}] \\ [G_{16}] & [G_{18}] - [G_{19}][G_{14}]^{-1}[G_{13}] \end{bmatrix}$$

$$[\tau_t] = \begin{bmatrix} [\tau_1] & 0 \\ 0 & [\tau_2] \end{bmatrix} \quad [I_t] = \begin{bmatrix} [I] & 0 \\ 0 & [I] \end{bmatrix} \quad [E_t] = \begin{bmatrix} E_x \\ E_y \end{bmatrix}$$

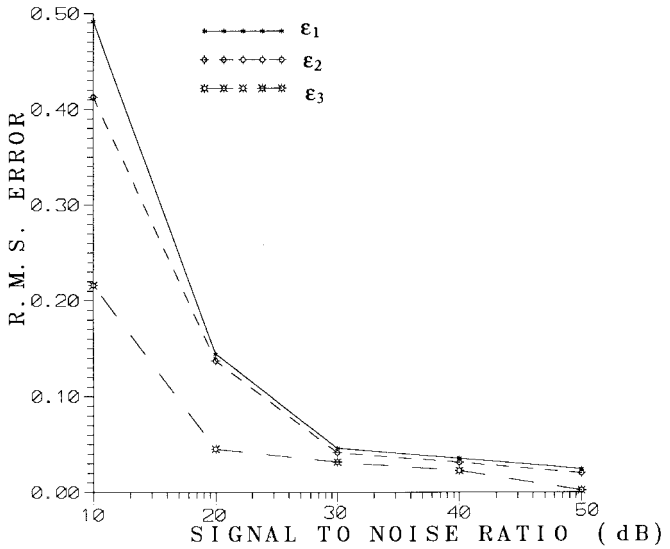

Fig. 7. Reconstructed error as a function of SNR for Example 2.

the following equations:

$$[\Psi_3][\tau_3] = [\phi_3] \tag{19}$$

$$[\Psi_t][\tau_t] = [\phi_t] \tag{20}$$

where

$$[\phi_3] = [E_p^s][E_p^i]^{-1}$$
$$[\Psi_3] = [E_p^s][E_p^i]^{-1}[G_{p1}] + [G_{p2}]$$
$$[\phi_t] = [E_t^s][E_t^i]^{-1}$$
$$[\Psi_t] = [E_t^s][E_t^i]^{-1}[G_{t1}] + [G_{t2}].$$

From (19), all the diagonal elements in matrix $[\tau_3]$ can be determined by comparing the element with the same subscripts which may be any row of both $[\psi_3]$ and $[\phi_3]$

$$(\tau_3)_{nn} = \frac{(\phi_z)_{mn}}{(\psi_z)_{mn}}$$

similarly, from (20)

$$(\tau_1)_{nn} = \frac{(\phi_t)_{mn}}{(\psi_t)_{mn}}, \qquad n \le N_1$$

$$(\tau_2)_{(n-N_1)(n-N_1)} = \frac{(\phi_t)_{mn}}{(\psi_t)_{mn}}, \qquad n \ge N_1 + 1.$$

Then the permittivities of each cell can be obtained as follows:

$$\varepsilon_{in} = (\tau_i)_{nn} + 1, \qquad i = 1, 2, 3.$$

Note that there are a total of M possible values of each element of τ_1, τ_2, and τ_3. Therefore, the average value of these M data is computed and chosen as final reconstruction result in the simulation. In the above derivation, the key problem is that the incident matrices $[E_p^i]$ and $[E_t^i]$ must not be singular matrices, i.e., all the incident column vectors that form the $[E_p^i]$ and $[E_t^i]$ matrices, must be linear unrelated. Thus, if the object is illuminated by a group of unrelated incident wave, it is possible to reconstruct the permittivity distribution of the materials. Note that when the number of cells becomes very large, it is difficult to make such a great number of measurements and on top of that make them all independent. As a result, the condition number of $[E_p^i]$ and $[E_t^i]$ is very large, i.e., the inversion of $[E_p^i]$ and $[E_t^i]$ is ill-posed. In such a case, some regularization method must be used to overcome the ill-posedness. For examples, the technique of pseudo-inverse transformation [1] can be applied for solving $[E_p^i]^{-1}$ and $[E_t^i]^{-1}$.

III. Numerical Results

The reconstruction of biaxial materials coated on a perfectly conducting cylinder illuminated by the beam focusing irradiation scheme is presented. Note that the shape of the conductor is given and the unknown is the permittivity distribution of the materials. The incident waves are generated by many groups of radiators operated outside the scatterers simultaneously. The incident wave from each group of radiators are to be restricted to a narrow bandwidth and this narrow bandwidth pattern can be implemented by antenna array techniques. Moreover, the beam sweeping for each group of radiators can be made by mechanical control or phase control. By changing the beam directions and tuning the phase of each group of radiators, one can focus all the incident beams in turn at each cell of the object. Plainly, an incident matrix formed in this way is diagonally dominant and its inverse matrix exists. This procedure is called the beam-focusing scheme [4]. Note that this focusing should occur when the scatterer being absent.

Some simulated results of two different examples are illustrated. The frequency of the incident wave is set to be 3 GHz and the number of illuminations is the same as cell's number. Four measurement points taken on a circle of radius 0.1 m at equal space are chosen for each illumination. Here we wish to emphasize that in order to avoid trivial inversion of finite-dimensional problems, it is crucial that the synthetic data generated through a direct solver are not alike to those obtained by the inverse solver. In our numerical examples, the discretization number for the direct problem is four times as that for the inverse problem.

In the first examples, the circular cross-section perfectly conducting cylinder coated with the circular cross-section penetrable inhomogeneous biaxial materials is presented. The radius of the conductor and the dielectric materials are 1 and 2.5 cm, respectively. The dielectric materials are discretized into 90 cells and their relative permittivities are plotted in Fig. 2. The model is characterized by simple step distribution of permittivities. Fig. 3 shows the reconstructed results. It is obviously that the reconstruction is good. The root mean square (rms) error is about 1.33, 2.03, and 0.83% for the permittivities ε_1, ε_2, and ε_3, respectively. The required CPU time for this examples is about 10 min on a SUN SPARC 20.

In the second example, the rectangular cross section of the composite materials coated on a rectangular cross-section conductor is discretized into 72 cells. The model is characterized by simple step distribution of permittivity in the x direction, five layer constant of permittivity in the y direction, and step distribution of permittivity in the z direction, as shown in Fig. 4. Each cell has 0.5 cm $\times$ 0.5 cm cross section. The reconstructed permittivity tensor distribution of the object are

plotted in Fig. 5. The rms error is about 1.85, 1.26, and 0.22% for the permittivities ε_1, ε_2, and ε_3, respectively. We can see that the reconstruction is also good.

In practice, the scattered field may be contaminated by random noise. For simulating the effect of noise, two independent values of Gaussian noise with zero mean are added to the real and imaginary part of the measured data, respectively. The signal-to-noise ratio (SNR) is defined as

$$S/N = 10\log[||\overline{E}^s(\overline{r})||^2/||N||^2] \quad \text{(dB)}.$$

The value of SNR used in the simulation includes 10, 20, 30, 40, and 50 dB. The numerical results for Examples 1 and 2 are given in Figs. 6 and 7, respectively. It shows the effect of noise is tolerable for SNR above 30 dB.

IV. Conclusions

An efficient algorithm for reconstructing the permittivity tensor distribution of the inhomogeneous biaxial materials coated on a given shape conductor has been proposed. By properly arranging the direction and the polarization of various unrelated incident waves, good reconstructed results have been obtained through simple matrix operations and the difficulty of the ill-posedness and nonlinearity is avoided. The moment method has been used to transform a set of integral equation into matrix forms. Then these matrix equations are solved by the unrelated illumination method. Numerical simulation for imaging the permittivity distribution of materials has been carried out and good reconstruction has been obtained even in the presence of Gaussian noise in measured data. Since no iteration is required, this algorithm is very efficient.

References

[1] M. M. Ney, A. M. Smith, and S. S. Stuchly, "A solution of electromagnetic imaging using pseudoinverse transformation," *IEEE Trans. Med. Imaging*, vol. MI-3, pp. 155–162, Dec. 1984.

[2] S. Caorsi, G. L. Grangnani, and M. Pastroino, "Redundant electromagnetic data for microwave imaging of three-dimensional dielectric objects," *IEEE Trans. Antennas Propagat.*, vol. 42, pp. 581–589, May 1994.

[3] T. M. Habashy and M. L. Oristaglio, "Simultaneous nonlinear reconstruction of two-dimensional permittivity and conductivity," *Radio Sci.*, vol. 29, pp. 1101–1118, July/Aug. 1994.

[4] W. Wang and S. Zhang, "Unrelated illumination method for electromagnetic inverse scattering of inhomogeneous lossy dielectric bodies," *IEEE Trans. Antennas Propagat.*, vol. 40, pp. 1292–1296, Nov. 1992.

[5] C. C. Chiu and P. T. Liu, "Image reconstruction of a complex cylinder illuminated by TE waves," *IEEE Trans. Microwave Theory Tech.*, vol. 44, pp. 1921–1927, Oct. 1996.

[6] N. Joachimowicz, C. Pichot, and J. P. Hugonin, "Inverse scattering: An iterative numerical method for electromagnetic imaging," *IEEE Trans. Antennas Propagat.*, vol. 39, pp. 1742– 1752, Dec. 1988.

[7] D. Colton and P. Monk, "A modified dual space method for solving the electromagnetic inverse scattering problem for an infinite cylinder," *Inverse Problems*, vol. 10, pp. 87–107, 1994.

[8] R. E. Kleinman and P. M. van den Berg, "A modified gradient method for two-dimensional problems in tomography," *J. Comput. Appl. Math.*, vol. 42, pp. 17–35, 1992.

[9] S. Barkeshli and R. G. Lautzenheiser, "An iterative method for inverse scattering problems based on an exact gradient search," *Radio Sci.*, vol. 29, pp. 1119–1130, July/Aug. 1994.

[10] R. F. Harrington, *Field Computation by Moment Methods.* New York: Macmillan, 1968.

[11] A. Ishimaru, *Electromagnetic Wave Propagation, Radiation and Scattering.* Englewood Cliffs, NJ: Prentice-Hall, 1991.

Chien-Ching Chiu was born in Taoyuan, Taiwan, ROC, on January 23, 1963. He received the B.S.C.E. degree from National Chiao Tung University, Hsinchu, Taiwan, in 1985 and the M.S.E.E. and Ph.D. degrees from National Taiwan University, Taipei, Taiwan, in 1987 and 1991, respectively.

From 1987 to 1989, he served in the ROC Army Force as a Communication Officer. In 1992 he joined the faculty of the Department of Electrical Engineering, Tamkang University, where he is now a Professor. His current research interests include microwave imaging and indoor wireless communications.